

Journal of Materials Chemistry B

Accepted Manuscript



This is an *Accepted Manuscript*, which has been through the Royal Society of Chemistry peer review process and has been accepted for publication.

Accepted Manuscripts are published online shortly after acceptance, before technical editing, formatting and proof reading. Using this free service, authors can make their results available to the community, in citable form, before we publish the edited article. We will replace this *Accepted Manuscript* with the edited and formatted *Advance Article* as soon as it is available.

You can find more information about *Accepted Manuscripts* in the [Information for Authors](#).

Please note that technical editing may introduce minor changes to the text and/or graphics, which may alter content. The journal's standard [Terms & Conditions](#) and the [Ethical guidelines](#) still apply. In no event shall the Royal Society of Chemistry be held responsible for any errors or omissions in this *Accepted Manuscript* or any consequences arising from the use of any information it contains.

ARTICLE

Hybrid Fullerene Conjugates as Vectors for DNA Cell-Delivery

Cite this: DOI: 10.1039/x0xx00000x

Cristina M. Uritu,^a Cristian D. Varganici,^a Laura Ursu,^a Adina Coroaba,^a Alina Nicolescu,^a Andrei I. Dascalu,^a Dragos Peptanariu,^a Daniela Stan,^b Cristina A. Constantinescu,^b Viorel Simion,^b Manuela Calin,^b Stelian S. Maier,^{a,c} Mariana Pinteala,^a Mihail Barboiu^{d*}

Received 00th January 2012,
Accepted 00th January 2012

DOI: 10.1039/x0xx00000x

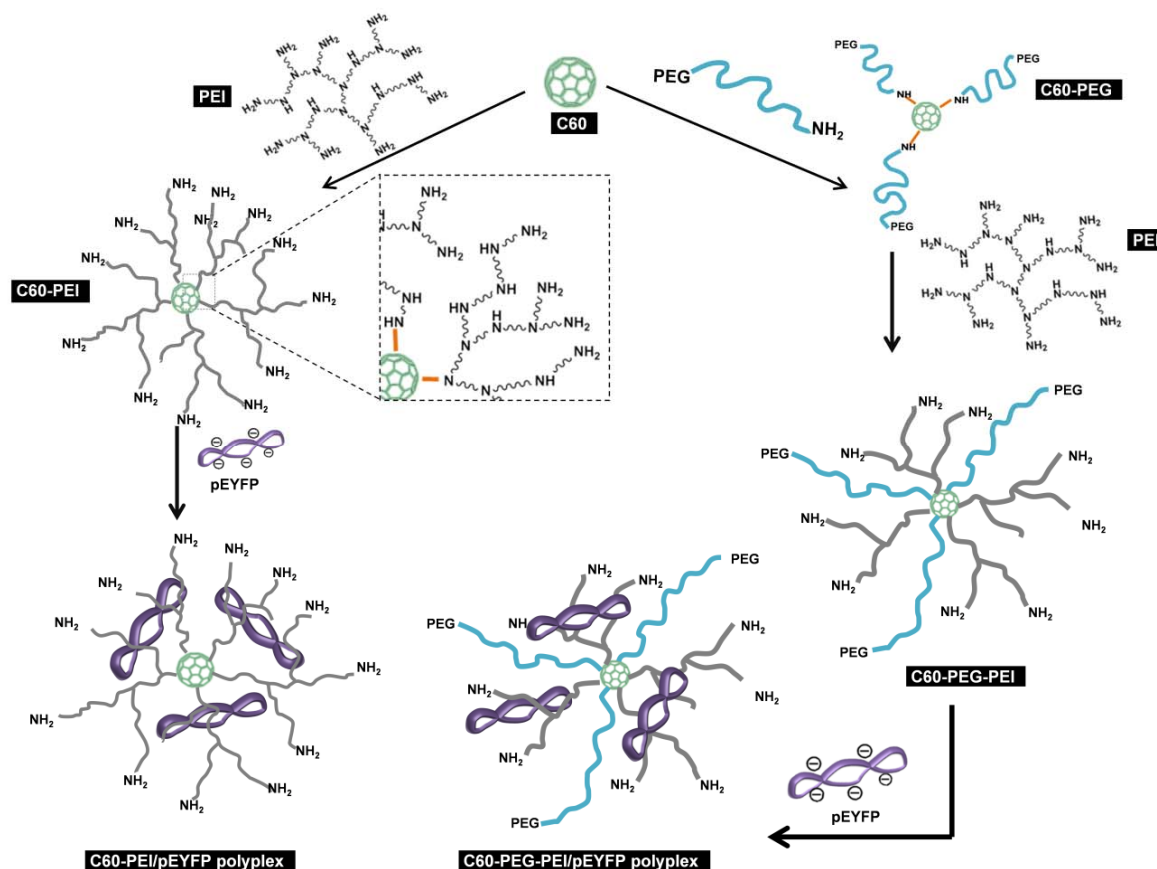
www.rsc.org/

The present study reports fullerene conjugates that act as efficient binders of double stranded DNA (dsDNA) into cytofriendly polyplexes. The conjugates are designed to generate dendrimeric structures, having C60 as the core and bearing linear or branched PEI and polyethyleneglycol (PEG) arms (~2kDa). Simple and reproducible synthesis pathways provided C60-PEI and C60-PEG-PEI conjugates. They were able to bind linear and plasmidic dsDNA and they form particulate polyplexes of 50 to 200 nm in diameter. The resulted polyplexes toggle between the anionic and cationic state at nitrogen to phosphorous ratios (N/P) of about 5, as revealed by their zeta potential and became colloiddally stable at N/P ratios above 10, as determined by atomic force microscopy (AFM). They are electrophoretically unbreakable starting with N/P ratios of 3 and of 5 when salmon sperm DNA and pEYFP-C1 plasmid, respectively are loaded. Both C60-PEI-pEYFP and C60-PEG-PEI-pEYFP polyplexes are non-cytotoxic against HEK 293T cells in culture and exhibit transfection efficiency better than 25% (N/P ratios above 20) and 6% (N/P ratios above 60) respectively, measured by flow cytometry. For comparison, the commercial SuperFect® from Qiagen (positive control) was able to provide an efficiency of 15-20%, under similar conditions. Moreover, the C60-PEG-PEI conjugate is as performant as the positive control in terms of expression of EYFP reporter gene in cultured cells and exhibited high cytocompatibility, determining cell proliferation up to 200%. Our study proved that C60-PEG-PEI is effective vector for DNA delivery being, in addition, easily synthesizable, practically non-cytotoxic and as efficient the commercially available transfection "tools."

Introduction

Replacing defective genes with fully functional copies by using gene therapy is one of the most promising techniques in modern medicine. Its basic approach is to selectively transfect DNA into affected cells, by making use of engineered viral or non-viral vectors. Three important features tend to prevail in preferring the use of non-viral vectors against viral ones: (i) the ability to control and to eliminate the occurrence of immunologic response to the carrying vector, (ii) the simplicity of use in transfection protocols and (iii) the ability to synthetically produce large amounts of vector-entities having highly reproducible structural and functional behaviours. Within this context, sterically exposed polycations are well suited to bind anionic DNAs *via* multiple ionic interactions, in a labile manner enough to act as reversible transporters. Even if cytotoxic *per se*, polyethyleneimines (PEI) having low-to-medium molecular weight (5 to 25 kDa) offer a good compromise in acting as DNA carriers.^{1,2} However, below 2 kDa they are unable to transfect cells, while becoming cytofriendly.³ Highly efficient and essentially nontoxic DNA carriers can be obtained by multivalent linking of short (0.8 kDa) PEI segments through polyacrylates, to build 14-30 kDa

conjugates.^{4a} However they are cytotoxic, PEGylated polymers have been used, however both toxicity and transfection efficiency are simultaneously reduced.^{4b} Concurrently, the design of hybrid nanosystems containing several functions like multivalent DNA binding sites, membrane penetration and anti-opsionisation functions has attracted a great deal of interest.⁵ Among them, fullerenes are unique platforms, but their biological applications are drastically limited by their extreme hydrophobicity, which minimizes their solubility in water. The C60 nanometric core is reactionally adaptive to various modifications, dimensionally well adapted to bind DNA targets and practically non-toxic.⁵⁻¹³ Water-soluble C60 fullerenes^{5c} have been used as antioxidant scavengers⁶, Glu-receptor antagonists⁷, neuroprotectants⁸, cell antiproliferatives⁹ and antineoplastic agents.^{10,11} Fullerene C60-PEI¹² and C60-polyamino¹³ conjugates have been effectively used in vitro and in vivo as DNA carriers with transfection efficiency and no acute toxicity, comparable to commercial reagents. The efforts have been focused on synthetic design approaches including the generation of hybrid structures allowing the binding and the membrane transport of the DNA and in the same time extremely important, to minimize toxicity.



Scheme 1. Synthetic routes for the C60-PEI and C60-PEG-PEI conjugates and their DNA polyplexes.

Polyethylene glycols (PEGs):PEIs conjugates have been used to reduce the cytotoxic potential.^{14,15} However, PEGylated systems are able to reduce immune response, but unfortunately, they also demonstrate low transfection ability, due to diminished cellular uptake and/or endosomal escape.^{16,17} In this paper we report effective fullerene-polyethylene-glycol-polyethyleneimine (C60-PEG-PEI) polyplexes showing high nucleic acid transfection efficiency with low toxicity, promoting cell proliferation. We report the synthesis and *in vitro* testing of a series of C60 fullerene-polyethyleneimine (C60-PEI) and C60 fullerene-polyethyleneglycol-polyethyleneimine (C60-PEG-PEI) conjugates acting as polyplex-type gene vectors for DNA delivery. Dendrimer-like structures of hyperbranched low molecular weight PEI (2 kDa) organized around a C60 fullerene hydrophobic core were considered. *In vitro* DNA binding and release tests were performed in two steps. First, by using salmon sperm dsDNA, the overall polyplex behavior of conjugates was certified in relation with their nitrogen to phosphorus, N/P ratios.^{18,19} Then, by using a plasmid carrying a reporter gene (pEYFP), the transfection ability of conjugates was proved, in cultures of HEK 293T cells which are able to replicate SV40 or bearing plasmids. The reporter gene encode the synthesis of an enhanced yellow-green fluorescent protein (EYFP) that exhibits bright green fluorescence when exposed to light in the blue to ultraviolet range. The expression of EYFP in HEK 293T cells confirms and quantifies the success of transfection. Interestingly, the C60-PEG-PEI conjugate, increase of

cellular proliferation compared to the C60-PEI and PEI samples.

Results and Discussion

Synthesis and characterization of C60-PEI and C60-PEG-PEI fullerene conjugates: Addition of aliphatic amines to C60 fullerene double-bonds *via* a nucleophilic addition mechanism has been reported and well documented.^{20,21} Herein, conjugation reactions involving the addition of amine-terminated PEG and PEI macromolecular precursors to unsaturated centers of fullerene were conducted at room temperature, in nonpolar solvents, in the presence of ambient light (see Experimental section, Scheme 1, Figures SI-1 and SI-2 in Electronic Supporting Information-ESI). The advancement of the addition reactions of PEI and PEG precursors to fullerene core was monitored by UV-VIS spectroscopy. UV absorption in 300-450 nm domain confirms the precursor addition to fullerene, by the time-vanishing of C60 specific peak ($\lambda=333$ nm) as a consequence of conjugate double-bonds consumption (see Figure SI-3 in ESI). Practically, after 24 h, the reaction is concluded.

The conjugation reactions have been evaluated by using different complementary methods. ¹H and ¹³C NMR, FTIR, and XPS spectroscopies are able to reveal the conversion of double bonds of fullerene in single bonds, concomitantly with the modification of the ratio between primary, secondary and tertiary amines of PEI and PEG substituents.

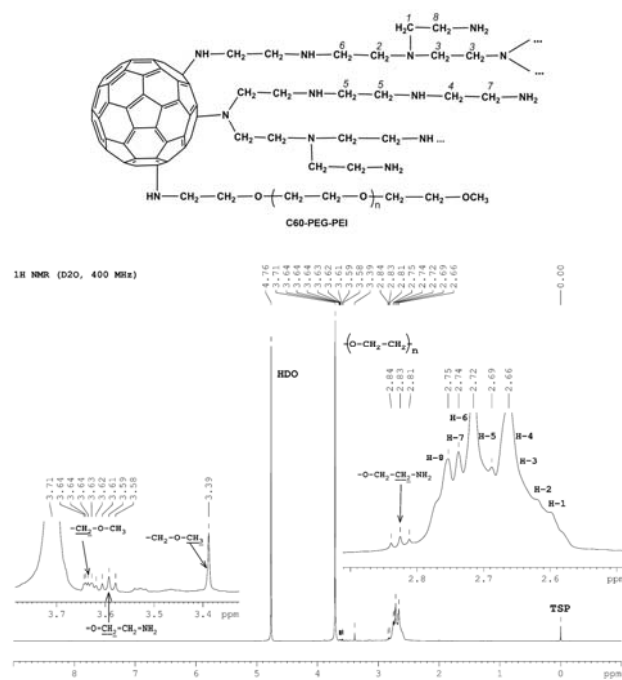


Fig. 1. ^1H -NMR spectrum of C60-PEG-PEI conjugate.

NMR experiments: To point out the effect of the addition of PEI and amino-PEG precursors to C60 fullerene, ^1H and ^{13}C NMR spectra of PEI and PEG reagents, together with the corresponding spectra of C60-PEI, C60-PEG, and C60-PEG-PEI conjugates have been used. (Figure 2 and Figures SI-4-9 in ESI). ^1H -NMR spectra of C60-PEI and C60-PEG-PEI conjugates are very similar to those of the precursor compounds. In the case of C60-PEI derivative, a downfield shift of 0.08 ppm (32 Hz) is observed for all the signals, as compared to the PEI spectrum, with almost all of the signals overlapping in interval 2.5-2.8 ppm.[‡] An obvious change can be observed for the broad signal corresponding to methylene protons from positions 7 and 8 in PEI structure, which now appears well separated from the rest of the signals (see comparatively Figures SI-4-8 in ESI and Figure 1). For the C60-PEG-PEI conjugate, the observed group of signals corresponding to the PEI moiety are practically unchanged. The signals corresponding to the PEG moiety exhibit different shifts, depending on their position: the signals of the methylene groups of the main chain (at 3.71 ppm) and by the end-chain MeO- groups (at 3.39 ppm) appears unaffected, while significant, upfield shifts of 0.20 and 0.40 ppm were obtained for the terminal O-CH₂-CH₂-NH-C60 methylene groups.[§]

^{13}C -NMR spectra of both C60-PEI and C60-PEG-PEI conjugates reveal the fullerene characteristic “fingerprint”, as a very broad low signal, in the 130-160 ppm region, corresponding to the *sp*² carbons (Figure SI-9 in ESI and Figure 2). The broadening of the *sp*² carbon signals can be assigned to fullerene asymmetry generated *via* addition of high molecular weight PEI and PEG precursors. Low upfield shifts, ranging from 0.20 up to 0.99 ppm (from 20 up to 100 Hz), were observed for all PEI signals of C60-PEI while they were practically unaffected in the case of C60-PEG-PEI. In the same manner as the discussed protons signals, the ^{13}C signals corresponding to the PEG moiety exhibit different modifications, depending on the position in the polymer structure.

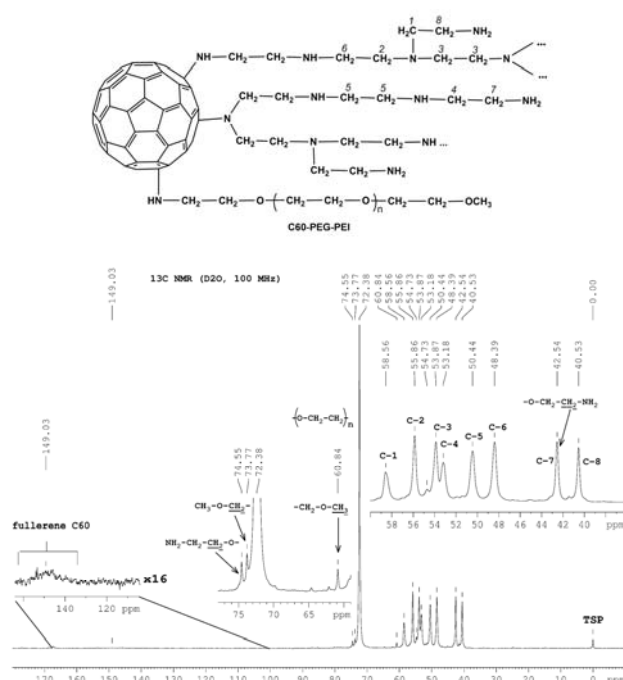


Fig. 2. ^{13}C -NMR spectrum of C60-PEG-PEI conjugate.

Thus, signals given by the methylene groups of the main chain (at 72.3 ppm), and of the MeO- groups (at 60.9 ppm), appear to be unaffected. Significant downfield shifts of 5.40 and 0.60 ppm, were noticed for the -O-CH₂-CH₂-NH- end group.[§] All these shifts can be attributed to the conversion of the primary amino groups into secondary amines, reminiscent with the grafting of PEI and PEG groups on the fullerene.

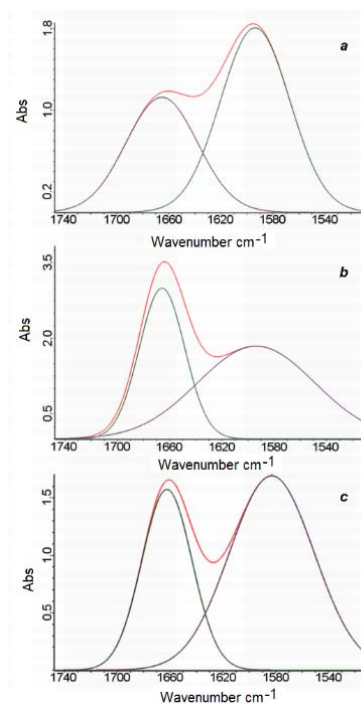


Fig. 3. Deconvoluted peaks of the FT-IR absorption bands of a) PEI precursor, b) C60-PEI and c) C60-PEG-PEI conjugates.

FT-IR experiments: Figures 3 and SI-10 in ESI show the FT-IR spectra of PEI and C60-PEI and C60-PEG-PEI conjugates. FT-IR spectra of PEI and PEI-C60 conjugate exhibit the characteristic bands for primary aliphatic

ARTICLE

Journal Name

amines at 3354 and 3289 cm^{-1} , while the weak band associated to secondary amines is positioned as a shoulder at 3432 cm^{-1} . Primary amines also absorb at 1659 cm^{-1} , while secondary amine groups absorb at 1597 cm^{-1} . The primary amine ($-\text{CH}_2\text{-NH}_2$) stretching absorption is weak and occurs at 1053 cm^{-1} , while the symmetric and asymmetric stretching of secondary aliphatic amines ($-\text{CH}_2\text{-NH-CH}_2-$) results in a moderate absorption at 1124 cm^{-1} . The strong bands at 2939, 2824 and 1460 cm^{-1} are attributed to the C-H stretching and rocking vibrations of ethylene moieties. The specific absorption bands for fullerenes are positioned at 523, 571, 1178 and 1425 cm^{-1} , and the stretching symmetric absorption band due to the conjugated double bonds ($-\text{C}=\text{C}-\text{C}=\text{C}-$) appears at 1630 cm^{-1} (weak). Bands due to both alkene and aromatic C-H stretching occur above 2962–2851 cm^{-1} . The FT-IR data are consistent with the PEI conjugation to C60 fullerene core, occurring preferentially through its primary amino groups.

This assertion is supported by the upfield shifts of FT-IR primary and secondary amine absorption bands from 1659 to 1663 cm^{-1} and respectively from 1597 to 1604 cm^{-1} . Specific secondary amine bands at 3354 and 3289 cm^{-1} show only minor modifications of their intensities and shapes, but no shifting. The presence of a broad band at 584 cm^{-1} in the spectrum of C60-PEI indicates the presence of C60. The FT-IR spectrum of C60-PEG-PEI conjugate presents the specific bands of secondary amine at 3354 and 3286 cm^{-1} and an upward-shifted primary amine band at 1663 cm^{-1} , as compared with that of free the PEI, located at 1659 cm^{-1} . The absorption of secondary amine band is up-shifted too, from 1597 to 1600 cm^{-1} due to the reaction of C60 with primary amine group of mPEG-NH₂. In the domain of C-H and $-\text{CH}_2$ stretching, a new band appears at 2885 cm^{-1} , due to the methylene groups of PEG chains. C60-PEG-PEI spectrum displays additional $-\text{C}-\text{O}-\text{C}-$ stretching bands, at 1280 and 1143 cm^{-1} . Deconvolution of FT-IR spectra in the range of 1740–1500 cm^{-1} (Figure 3) allows the comparison of characteristic ratios between the peaks area of primary and secondary amine. In the case of PEI precursor, the calculated ratio is 0.64. It decreases to 0.60 and 0.55 when calculated for C60-PEI and C60-PEG-PEI FT-IR conjugates, respectively. Such a decrease is reminiscent with the conversion of the primary amino groups into secondary ones, which confirms that fullerene reacts mainly with primary amino end-groups of PEI and PEG precursors.

X-ray photoelectron spectrometry-XPS experiments:

The reaction between C60 and PEI and PEG precursors is also confirmed by high resolution XPS spectra. Figure SI-11 and Table SI-1 in ESI, describe the wide scan spectra of PEI, C60-PEI, C60-PEG-PEI, and PEG, respectively. The peaks of binding energies of 285 and 398 eV were assigned to C 1s and N 1s. The presence of O 1s, even in small percentage, at a binding energy of about 530 eV can be noticed in spectra of PEI precursor and of C60-PEI conjugate probably due to the incomplete removal of water during lyophilization. The percent of elemental carbon in C60-PEI and C60-PEG-PEI samples increases as compared with the values in PEI or/and in PEG (Figure 4). The high resolution C 1s peak between 284.2 eV and 286.2 eV observed for the C60-PEI sample, was resolved in four

characteristic deconvoluted peaks, attributed to C=C, C-C/C-H, C-N and C-NH bonds, respectively. The same C 1s peak of C60-PEG-PEI, ranged between 284.4 eV and 287.1 eV, reveal one more deconvoluted peak, characteristic for the C-O bond of PEG. The N 1s peak was resolved in four deconvoluted peaks, assigned to N-C, N-H, HN-C and NH₂ chemical groups in all PEI-containing conjugates (Figure 4), confirming their structure, and their cationic state. Elemental compositions calculated based on the wide scan XPS spectra of investigated precursors (PEI and PEG) and of conjugates (C60-PEI and C60-PEG-PEI) are resumed in Table SI-1 in ESI. Tabulated data permit to numerically estimate the compositional ratios of the components in C60-based conjugates. The ratio of C60 : PEI is 1:3.5 for C60-PEI, and 1:2.5 for C60-PEG-PEI, respectively, and the C60 : PEG ratio is 1 : 0.9 for C60-PEG-PEI.

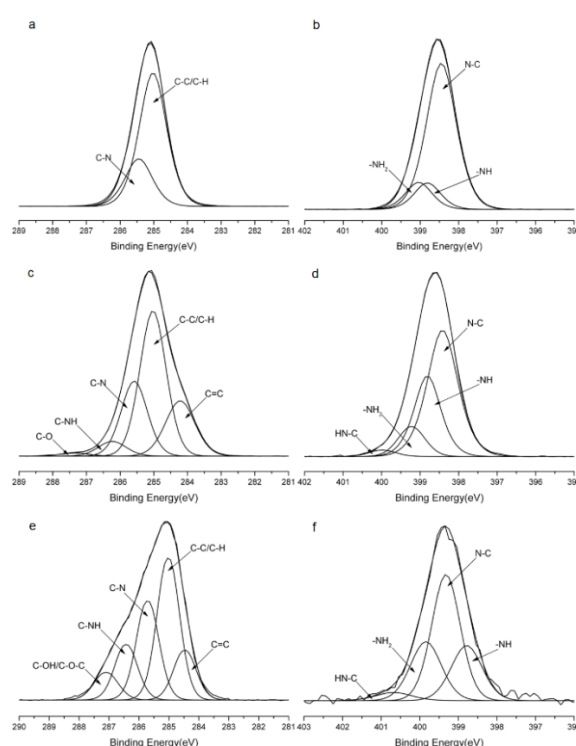


Fig. 4. Deconvoluted high resolution XPS spectra of C 1s (left column) and N 1s (right column) of PEI (a and b), C60-PEI (c and d), and C60-PEG-PEI (e and f).

Thermal Analysis experiments: Thermal analysis emphasizes the covalent bonding between C60 and PEI and PEG terminated amines (Figure SI-12 in ESI). PEI thermally degrades in three individual decomposition stages: the first ranging between 50–185°C (8% mass loss) corresponds to loss of ammonia, continues with ethylamine evolution in the second stage between 270–345°C (25% mass loss) and following with the formation of pyrrol and C-substituted ethylpyrroles in the third stage (65% mass loss) in the range 350–420°C.²⁴ The first thermal decomposition stage of C60-PEI conjugate shows two distinct processes, attributed to solvent traces and ammonia elimination. Covalent PEI addition to C60 fullerene is indicated by the disappearance of the second degradation stage and by the significant increase of residual mass percentage at (700°C) from 1.25% observed for PEI to 9.18% determined for C60-PEI conjugate. Following the

procedure described by Shi and co-authors,²² a ratio of 3.5 moles of PEI to 1 mole of C60 has been determined based on 98% and 91% (excluding the 5% solvent traces) mass losses at 420°C observed for PEI and C60-PEI respectively, which is in perfect agreement with the ratio values determined by the XPS. DSC analysis show that PEI exhibits a typical glass transition temperature domain (T_g) at -57°C while the C60-PEI shows a higher T_g , at -52°C (Figure SI-13a in ESI), attributed to the reduction of the free volume between PEI chains, owed to segmental chain stiffening caused by steric hindrance. The intense exothermic peak at 160°C is reminiscent to a packing crystallization phenomenon of C60-PEI, leading to the formation of a cluster-like nanostructures, which narrows distances between PEI chains. On the second heating run, the T_g significantly increases to nearly 0°C, indicating a higher packing degree of PEI chains in the structure of C60-PEI conjugate. On the other hand, free mPEG-NH₂ exhibits a barely perceptible T_g transition, with a value centered at -55°C, and a characteristic melting process with a temperature peak value of 58°C and an enthalpy value of 180 J/g (Figure SI-13b in ESI).

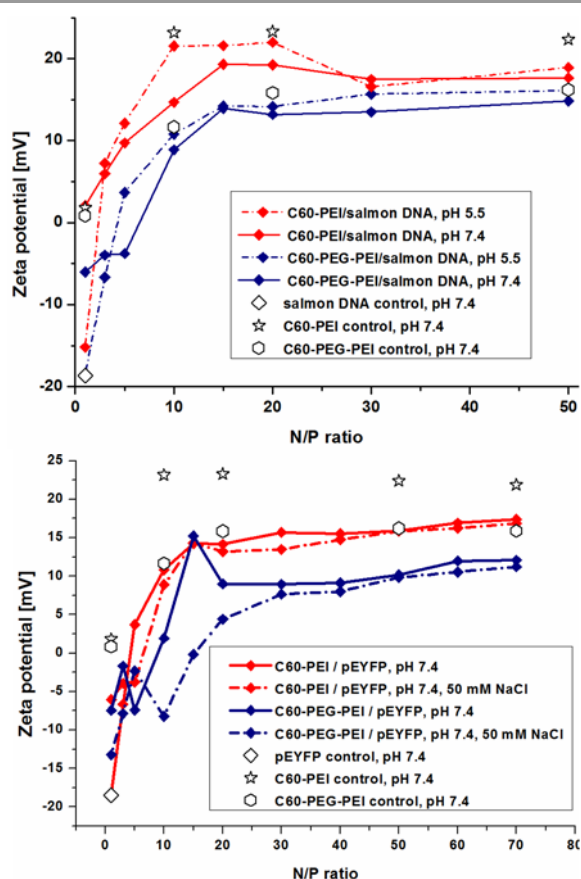


Fig. 5. Zeta-potential of the particulate polyplexes of a) salmon sperm dsDNA and b) pEYFP DNA function on the N/P ratios. Zeta potential values are depending on the concentration of conjugate, ranging between around 2 and 23 mV for C60-PEI conjugate when the concentration varied between 0.012 and 0.72 g/L. When the concentration of C60-PEG-PEI varied between 0.06 and 0.75 g/L zeta potential varies between 0.8 and 16 mV. dsDNA and pEYFP concentrations were constant (0.034 g/L dsDNA and 1.173 mg/L pEYFP), and zeta potential was around -20 mV.

For the C60-PEG-PEI sample a unique T_g transition, centered at -40°C can be observed indicating a good phase miscibility and which is higher than that of PEI (-57°C) and PEG (-55°C) amino-precursors. Probably, PEG is able

to significantly reduce the crystalline morphology and the structural packing capacity of PEI. A supplemental confirmation is provided by the obvious decrease of the temperature peak in the melting profile of C60-PEG-PEI (54°C), in comparison with that of mPEG-NH₂ (58°C) and by the significant decrease of C60-PEG-PEI melting peak ($\Delta H = 62$ J/g, as compared to $\Delta H = 180$ J/g of mPEG-NH₂ precursor).

DNA polyplexes based on the C60-PEI and C60-PEG-PEI conjugates.

Two types of polyplexes of C60-PEI and C60-PEG-PEI conjugates were produced by mixing conjugates and dsDNA and characterized by using a linear dsDNA (salmon sperm DNA; ~200 base pairs) and a circular dsDNA (pEYFP-C1 plasmid; ~4700 base pairs). All related studies were performed considering compositions precisely formulated between the carriers and the dsDNA, calculated as ratios between the molar fraction N/P of nitrogen in the C60-based conjugates and the molar content of phosphorous in the nucleic acids. To determine the colloidal stability of the polyplexes in aqueous solutions, the zeta potential of the particulate polyplexes (resulted by carrier – dsDNA association) was investigated using the Dynamic Light Scattering (DLS) technique. Figure 5 summarize the results of zeta-potential measurements performed on the polyplexes of increasing N/P ratios. Supplemental dependences on pH and ionic strength were also considered. As expected the results were indicate that the polyplexes are cationic for N/P ratios from 3 to 10, depending on the ionic strength. Above these values, several conjugate molecules “collaborate” to electrostatically neutralize negative charges of dsDNA within the same particle, resulting in a positive overall charge. Even at large N/P ratios (at least up to a value of 50), polyplexes preserve their unitary particulate characteristics (their overall positive charge is still slowly increasing).

Morphological and dimensional behaviors of C60-PEI and C60-PEG-PEI conjugates and their corresponding pEYFP plasmid polyplexes were investigated by Atomic Force Microscopy (AFM).

Figure 6 resume the imaging results and the particles mean size dispersion determined by AFM. Samples were prepared from mixtures of 1 μ g dsDNA in 20 μ L solution of 1X TAE buffer (pH 7.4) and the variable amounts of C60-based conjugates for different N/P ratios. After one hour incubation time, 10 μ L of each resulted suspension were deposited on freshly cleaved mica substrates, rinsed with water and air dried, at room temperature. To put in evidence the relations between the composition and the morphologic behaviours of polyplexes and to avoid artifacts due to carriers self-assembling, the AFM analyses presented in Figure 6 were performed on near-neutral or low cationic polyplexes, having a well-defined composition and a N/P ratio equal to 10. From the analysis of the AFM images, it is obvious that polyplexes have a more compact structure as compared with the C60-PEI and C60-PEG-PEI carriers. The latter ones tends to self-assemble into large, loose clusters, highly hydrated in aqueous medium, having dimensions correlated with the abundance of cationic amino groups (mean diameters of ~207 nm for C60-PEI and of ~69 nm for C60-PEG-PEI).

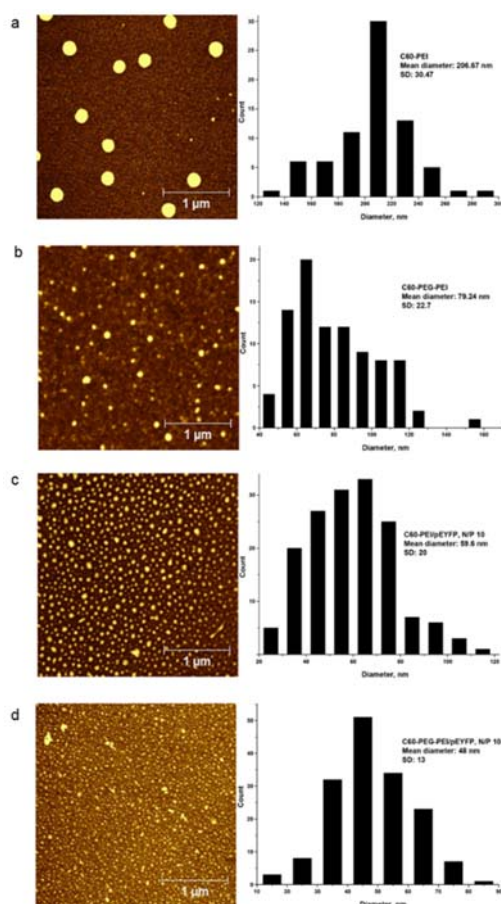


Fig. 6. Atomic force microscopy images (left) and particles diameter distribution (right) of a) C60-PEI and b) C60-PEG-PEI conjugates and of their corresponding polyplexes c) C60-PEI · pEYFP plasmid and d) C60-PEG-PEI · pEYFP plasmid at a N/P ratio of 10.

The particles resulted by the complexation of C60-based conjugates with the pEYFP plasmid are denser packed,

even if they are more complex in structure. For investigated polyplexes having different N/P ratios (not shown here), particles size did not exceed 500 nm in none of the cases, regardless the pH or ionic strength of the suspension.

The dsDNA binding ability of C60-PEI and C60-PEG-PEI conjugates was investigated by agarose gel electrophoresis. Figure 7 shows electrophoretic lanes of free dsDNA and of C60-PEI · salmon sperm dsDNA, C60-PEG-PEI · salmon sperm dsDNA, C60-PEI · pEYFP and C60-PEG-PEI · pEYFP polyplexes having different N/P ratios. The concentration of nucleic acids was kept constant at 1 µg/well. A difference can be noticed between the conjugates ability to condense flexible, lower weight salmon sperm dsDNA and the stiffer, higher weight plasmid dsDNA. In this respect, a leveling effect is obvious in the case of C60-PEI carriers, while C60-PEI-PEG is less effective in binding plasmidic dsDNA. Retardation assay performed for pEYFP plasmid polyplexes exhibits more complex behaviors: the plasmid folding/twisting/coiling peculiarities is revealed by the migrating multiple spots of topologically-distinct forms (supercoiled form migrate faster comparing with nicked circle form). When compared to the free pEYFP, the migration of plasmid is completely blocked for N/P ratios higher than 5, in the case of C60-PEI · pEYFP polyplex and higher than 10, in the case of C60-PEG-PEI · pEYFP polyplex, respectively. By contrast, in the case of linear salmon sperm dsDNA, polyplex migration is practically blocked at a N/P ratio equal to 3. A better packing between the plasmid and C60-PEG-PEI conjugate takes place at a N/P ratio higher than those used for C60-PEI, as a consequence of the presence of PEG chains, which diminish the PEI capacity to complex the nucleic acids.

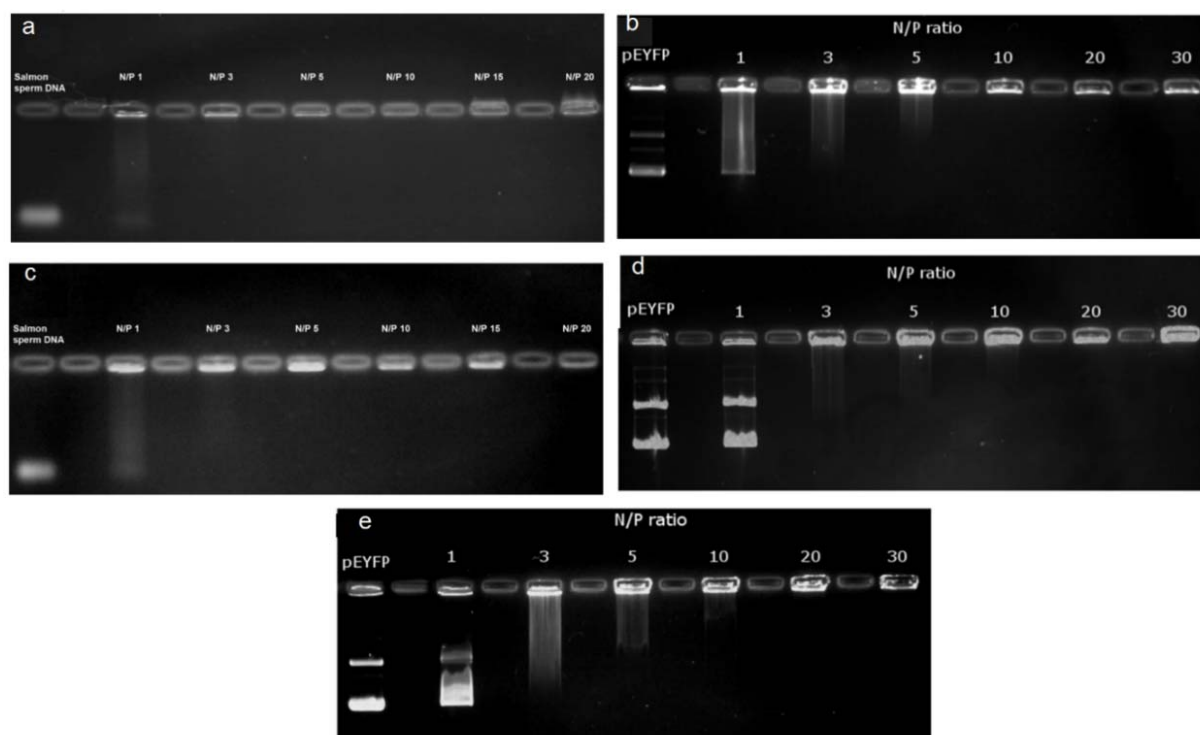


Fig. 7. Agarose gel retardation assays in the case of a) C60-PEI · salmon sperm dsDNA, b) C60-PEI · pEYFP plasmid c) C60-PEG-PEI · salmon sperm dsDNA, d) C60-PEG-PEI · pEYFP plasmid and e) PEI · pEYFP plasmid polyplexes at different N/P ratios.

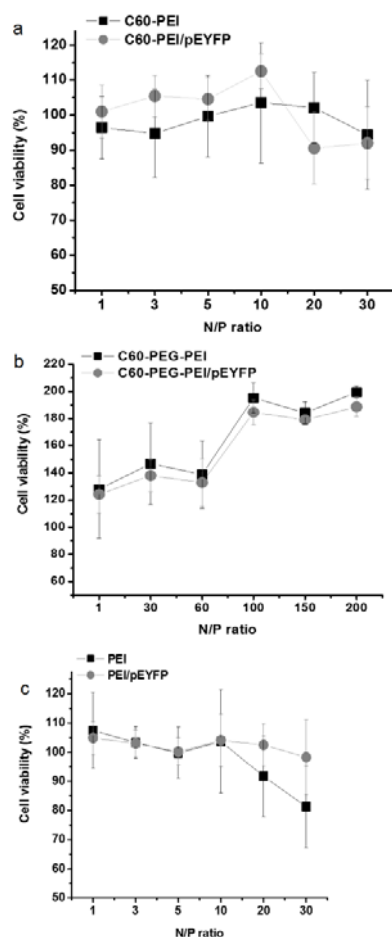


Fig. 8. The viability of HEK 293T cells in the presence of a) C60-PEI and b) C60-PEG-PEI, and their polyplexes with pEYFP plasmidic dsDNA in comparison with c) their viability after contacting with PEI 2 kDa and the PEI/pEYFP polyplex. The reference conjugates have been tested by using as same amounts as used for polyplexes at different N/P ratios.

In the case of C60-PEI-pEYFP polyplex, the increasing of N/P ratios determines a decrease of pEYFP visible in the loading well, suggesting a very good packaging and protection of pEYFP by the C60-PEI carrier, which prevents the plasmid staining by ethidium bromide. Comparatively, regardless the N/P ratio value, in the case of polyplex formed between naked PEI and pEYFP, the plasmid DNA can be observed in the loading well, indicating the incapacity of PEI to efficiently wrap and protect pEYFP.

The cytotoxicity of C60-PEI and C60-PEG-PEI conjugates and of their plasmidic pEYFP polyplexes

was investigated on HEK 293T cell cultures, using the MTT assay –see Experimental section for details (Figure 8). The viability of HEK cells grown in DMEM culture medium, in the presence of free PEI, of C60-PEI and of C60-PEG-PEI conjugates, and of their corresponding polyplexes with pEYFP plasmid at different N/P ratios, was determined, in triplicate, with reference to control samples (cells grown in DMEM culture medium). The concentration of pEYFP was kept constant at $1\mu\text{g}/\text{mL}$ and the concentration of the conjugate was varied so as to obtain the N/P ratios of interest. In all cases, the viability of HEK 293T cells is appropriate for the envisioned application in cell transfection. A cellular viability higher than 95 % was obtained for both uncomplexed C60-PEI

and its polyplexes with pEYFP, for N/P ratios up to 10 (Figure 8a). A relative lower viability, of about 90 %, was noticed for N/P ratios of 20 and 30. Interestingly, in the case of C60-PEG-PEI conjugate, the presence of hydrophilic PEG chains determined an increase of cellular proliferation compared to the control samples, regardless the N/P ratios. The proliferation increase is proportional with the increasing of N/P ratio, being double for a N/P ratio of 200 (Figure 8b). In the case of 2 kDa PEI, either uncomplexed or complexed with pEYFP, no negative effect on cellular viability was noticed up to a N/P ratio of 10. Above this value, free PEI induces a decrease of cellular viability with about 20%, whereas the PEI/pEYFP polyplexes remain highly cytofriendly (Figure 8c).

The transfection efficiency of the polyplexes based on the synthesized conjugates was determined by two complementary techniques: i) the fluorescence microscopy, to qualitatively evaluate the abundance of transfected cells and ii) the flow cytometry, to quantitatively measure the transfection yield (Figures 9 and 10). Both techniques have benefited from the use of pEYFP-C1 plasmid vector, taking advantage of the reporter gene included in the plasmid, which triggers the expression of genetically engineered enhanced yellow-green *Aequorea victoria* fluorescent protein (EYFP). Negative control (cells cultured in normal conditions) and positive control (cells transfected using SuperFect® reagent kit, from Qiagen) are also performed.

The results prove an obvious dependence of EYFP expression on the type and N/P ratio of the polyplexes. The fluorescence of transfected HEK 293T cells at different N/P ratio of C60-PEI-pEYFP, C60-PEG-PEI-pEYFP and PEI-pEYFP polyplexes was directly observed after 48 hours under a fluorescence microscope and the transfection efficiency was determined by flow cytometry, as the percent of cells that express the fluorescent protein relative to the total number of counted cells. The measured values of mean fluorescence intensity (MFI) reflect the expression level of fluorescent protein of each transfected cell. The flow cytometry data for different N/P ratios of C60-PEI-pEYFP, C60-PEG-PEI-pEYFP and PEI-pEYFP polyplexes are presented in Figure 10, as percent of transfected cells, and as mean fluorescence intensity. As showed in Figure 10, C60-PEI-pEYFP polyplex started to transfect at a N/P ratio of 1, but the maximum transfection efficiency was obtained for N/P ratios between 10 and 20, while C60-PEG-PEI-pEYFP is efficient only at N/P ratios above 60. Up to a N/P ratio of 10, the percent of transfected cells and the mean fluorescent intensity-MFI values obtained for C60-PEI-pEYFP polyplexes increase with increasing N/P ratio. Above that, no statistically significant increase could be obtained (percent transfected cells was 20% at N/P=10 and 28.76 % N/P=30). In the case of C60-PEG-PEI/pEYFP polyplexes, reasonable transfection yields were obtained for N/P ratios above 60 (percent transfected cells was 6.3% at N/P=60 and 10.6 % at N/P=200) as compared with C60-PEI-pEYFP, and a discrepancy between the relative amount of transfected cells and the MFI values becomes obvious, almost the same as observed for C60-PEI-pEYFP polyplexes at N/P=20, 30 and positive control experiment with the

commercial product (Figure 10a,b). The lower transfection efficiency of C60-PEG-PEI-pEYFP in comparison with C60-PEI-pEYFP can be explained by the presence of PEG chains in the structure of the carrier, which may hinder the proper packaging of plasmid by covering the surface of the conjugate.^{16,17} Comparatively, the high MFI measured values (of about 1800, versus 25 in control untreated cells) suggests a higher efficiency of protein expression in the cells transfected with C60-PEG-PEI-pEYFP polyplexes (Figure 10a,b). The size and zeta potential values measured for N/P ratios above 5, for C60-PEI-pEYFP and above 60 for C60-PEG-PEI-pEYFP, are around 50-100 nm, and 10-20 mV, respectively (Figures 5 and 6). This fact is in good agreement with the optimal values of size and zeta potential for efficient gene delivery, reported in literature.¹⁶

The use of PEI-pEYFP polyplexes resulted in modest transfection yields at any given N/P ratio (Figure 10c). The comparison of MFI values, which are a measure of the expression level of fluorescent protein in each transfected cell, reveals that C60-PEI-pEYFP and C60-PEG-PEI-pEYFP polyplexes are 36 and respectively 40 folds more effective in comparison with PEI-pEYFP. A possible explanation of this result is that the presence of the hydrophilic PEG may impede the intracellular delivery of the polyplexes and as a consequence the number of cells that take up the polyplexes is reduced as compared with the case of using non-PEGylated-PEI conjugate. Thus, the cells that cope to internalize the polyplexes are able to express the fluorescent protein at high levels (reflected by MFI, expressed as fluorescence arbitrary units).

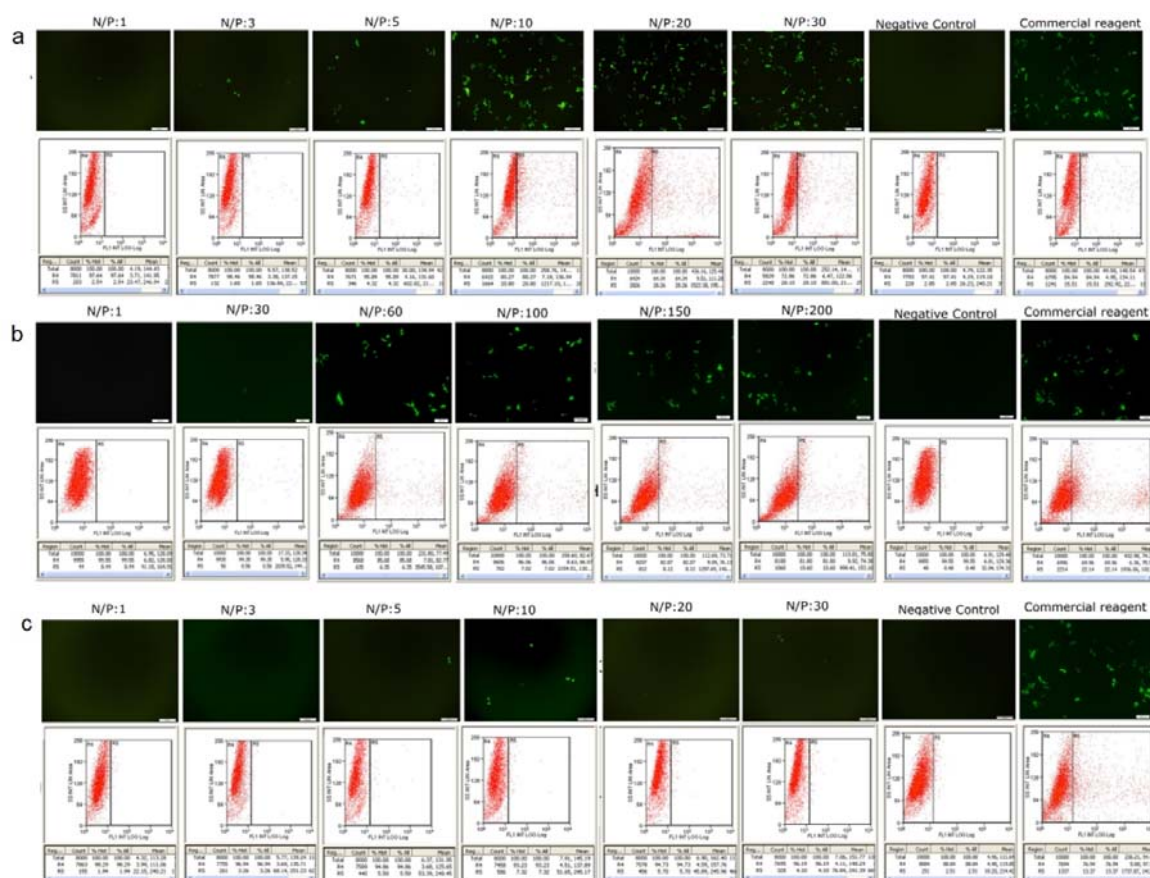


Fig. 9. Expression of EYFP in HEK 293T cells transfected with a) C60-PEI-pEYFP, b) C60-PEG-PEI-pEYFP and c) PEI-pEYFP polyplexes at different N/P ratios, as revealed, 48 hours post-transfection, by fluorescence microscopy (scale bar 200 μm) and by flow cytometry analysis.

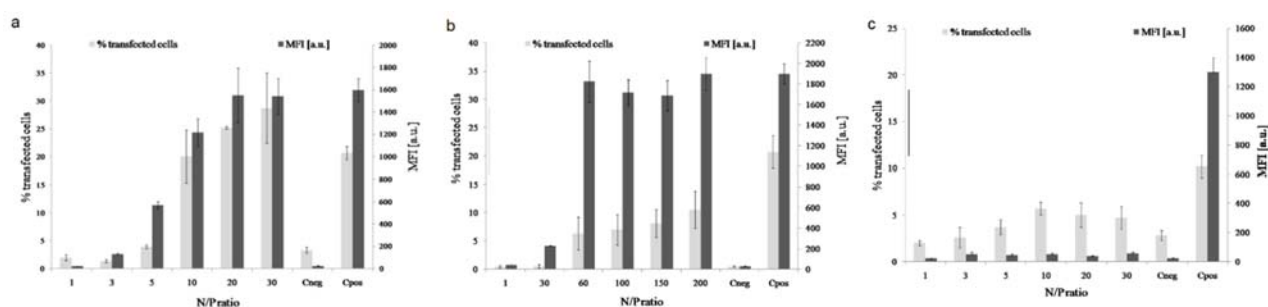


Fig. 10. Transfection efficiency by mean fluorescence intensity of a) C60-PEI-pEYFP, b) C60-PEG-PEI-pEYFP and c) PEI-pEYFP polyplexes at different N/P ratios, expressed by transfection percentage rate.

ARTICLE

To facilitate comparisons of flow cytometry data (Figures 9 and SI-14-16 (in ESI) include representative images and values for the negative control (cells incubated with cell culture medium only) and positive control (HEK 293T cells transfected using a commercial reagent, SuperFect® from Qiagen, at its optimal working condition based on the producer's instructions). It is obvious that, for N/P ratios 10, 20, and 30, C60-PEI polyplexes are more effective in inducing transfection than SuperFect® commercial nucleic acids carrier.

Using the C60-PEI and C60-PEG-PEI vectors synthesized by us, equivalent transfection efficiencies were obtained in comparison with results recently reported in literature.^{13,23} Working with G2 PAMAM dendrimers, Liu, Wang et al. transfected HEK 293T cells with a mean efficiency of 34.8%, for a N/P ratio of 40, when EGFP plasmid was vectorised. Similar results, but at lower N/P ratios, are provided by our C60-PEI conjugate. Relative to G2 PAMAM dendrimers, better cytocompatibility were obtained for both C60-PEI and C60-PEG-PEI conjugates, with a significant improved cytotoxic properties in the case of C60-PEG-PEI-pEYFP polyplexes having N/P ratios higher than 60.

Conclusions

The present study describes the synthesis and characterization of a class of DNA carriers based on conjugates of C60 fullerene with 2kDa branched PEI, optionally supplemented with 2kDa PEG, to potentially increase their cytotoxicity. Following a simple and reproducible synthesis pathway, conducted in anhydrous solvents, at ambient temperature and lighting, under nitrogen atmosphere, C60-PEI conjugates having a molar ratio of 1:3.5, and C60-PEG-PEI conjugates with compositional ratios of 1:0.9:2.5, were obtained. The conjugates are able to act as gene vectors, by forming stable polyplexes with linear or plasmidic dsDNA (2kbp salmon sperm DNA, and 4.7kbp pEYFP-C1, were tested). Depending on the type and amount of associated DNA, polyplexes have particulate dimensions, ranging between 50 and 200 nm. Depending on the N/P ratio, C60-PEI-pEYFP and C60-PEG-PEI-pEYFP polyplexes exhibit transfection efficiency above 25% and 6% respectively; the C60-PEI-pEYFP polyplex showed a slightly higher transfection efficiency, as compared with SuperFect® commercial reagent (15%). In the case of the second conjugate (C60-PEG-PEI), the lower transfection efficiency could be compensated, in real applications, by the benefits of PEGylation toward low cytotoxic agents. The C60-PEG-PEI conjugate is as performant as the positive control in terms of expression of EYFP reporter gene in cultured cells and more importantly exhibited better cytocompatibility, determining high cell proliferation up to 200%.

These findings may provide insight in the development of multifunctional adaptive vectors carrying out several functionalities for for optimal DNA binding, membrane penetration, DNA delivery and anti-opsonisation functions.

Next important application problems, deriving from the enormous variability of both DNA targets and nature of the transfected cells, the rational design will become limited to the introduction of a reduced number of components and should be completed by combinatorial approaches. Within this context, the Dynamers²⁴ or Dynamic Reversible Frameworks²⁵ might be considered as an attractive screening systems for the rapid access to the active systems from large and complex arrays. Work is in the progress to further develop such dynamic adaptive systems.

Experimental

Materials. Fullerene-C60 (sublimed, 99.9%) and branched polyethylenimine (PEI, average $M_w=2kDa$, 50 wt% in H₂O) were purchased from Sigma-Aldrich (St. Louis, MO, USA). α -(2-aminoethyl)- ω -Mepolyethyleneglycol (mPEG-NH₂, average $M_w=2kDa$), was purchased from JenKem Technology (Allen, TX, USA). DNA (low molecular weight, salmon sperm) was purchased from Fluka (St. Louis, MO, USA). Plasmid pEYFP was purchased from Clontech Laboratories Inc. (Mountain View, CA, USA) and the Plasmid Midi Kit from Qiagen (Düsseldorf, Germany). 3-[4,5-dimethylthiazol-2-yl]-2,5-diphenyltetrazolium bromide (MTT) was purchased from Sigma-Aldrich Chemie (Germany). Dulbecco's modified Eagle's medium (DMEM), fetal calf serum (FCS), penicillin G, neomycin, streptomycin were purchased from Gibco BRL (Gaithersburg, MD, USA), and the cell culture plates from Corning (New York, NY, USA).

Synthesis of C60-PEI. 0.12 g (0.16 mmol) of C60 fullerene was dissolved in 450 mL chloroform, under nitrogen atmosphere. After 4 hours stirring, a magenta-colored mixture was obtained. To this solution, 3.33 g (1.66 mmol) of branched PEI (M_w 2 kDa) previously suspended in 100 mL chloroform, was added. The reaction mixture was maintained under continuous stirring for 5 days. All synthesis steps were carried at ambient temperature and lighting, under nitrogen purging. To evaluate the reaction progress, UV-Vis analyses were performed at specific time intervals, tracing the disappearance of the peak at 330 nm. The reaction product was isolated by removing the solvent in two steps: firstly by using a rotary evaporator (25°C, 20 mmHg), and secondly under high vacuum (22°C, 0.33 mmHg). Further, the C60-PEI product was dissolved in a small amount of deionized water, and the solution was dialyzed for 7 days with deionized water, using a Spectra/Por 7 dialysis membrane (3.5 kDa MWCO, Spectrum Laboratories Inc.), with daily water change. Finally, the dialyzed solution was lyophilized, and 2.5 g of C60-PEI were obtained.

Synthesis of PEGylated C60-PEI. 0.025 g (0.0347 mmol) of C60 fullerene was dissolved in 30 mL toluene, under the same conditions as those described for C60-PEI synthesis. To this

solution, 0.1388 g (0.0694 mmol) of methoxy-PEG-amine HCl salt (mPEG-NH₂, M_w 2 kDa) previously dissolved in 10 mL chloroform was added, and the mixture was maintained under continuous stirring, at ambient temperature and lighting, under nitrogen atmosphere. The reaction progress was monitored by UV-Vis spectroscopy. After 5 days, 0.6944 g (0.3472 mmol) of branched PEI solution in 10 mL chloroform was added, and the reaction mixture was further maintained under stirring for another 5 days, under the same ambient conditions, in oxygen-free environment. The isolation and purification of the reaction product were performed in the same way as those described in the case of C60-PEI synthesis, and 0.6 g of C60-PEG-PEI were obtained.

Synthesis of C60-PEI/DNA and C60-PEG-PEI / DNA polyplexes. Based on the amount of nitrogen contained by 1 μg of PEI, C60-PEI and C60-PEG-PEI conjugates (previously determined by XPS and confirmed by EDX) and considering that 1 μg of dsDNA contains 3 nmol of phosphorus, polyplexes having different nitrogen/phosphorus molar ratios (N/P) were prepared as following: aqueous solutions of conjugates and salmon sperm DNA or separately plasmidic DNA (pEYFP) were mixed and after gentle vortexing (to avoid the temperature rises above 35°C), mixtures were maintained at room temperature for 30 minutes.

NMR Spectroscopy: NMR spectra have been recorded on a Bruker Avance III 400 instrument operated at 400.1 and 100.6 MHz for ¹H and ¹³C nuclei, respectively, at 25°C. 1D NMR signal assignments were done based on 2D NMR homo- and heteronuclear correlations (not shown here). H,H-COSY, H,C-HSQC and H,C-HMBC experiments were recorded using standard pulse sequences, in the version with z-gradients, as delivered by Bruker with TopSpin 2.1 PL6 spectrometer control and processing software. The spectra of PEI and PEG precursors were recorded on a 5 mm four nuclei (QNP) direct detection, z-gradient probe while the spectra of the final C60-PEI and C60-PEG-PEI conjugates were recorded on a 10 mm multinuclear direct detection, z-gradient probe, to overcome the low concentration of fullerene moiety. All samples were dissolved in D₂O. Chemical shifts were reported in ppm, and referred to 3-(trimethylsilyl)propionic-2,2,3,3-d₄ acid sodium salt (TSP) as internal standard.

PEI exhibits a complicated ¹H NMR spectrum, with almost all of the signals overlapping in interval 2.5-2.8 ppm. This makes the exact assignments (shape of the signals and the corresponding number of protons) very difficult to assess. Thus, for individual PEI and for both C60 PEI-containing conjugates, we describe herebelow only the proton chemical shifts, extracted from the 2D ¹H-¹³C HSQC spectra.

PEI: ¹H-NMR (D₂O, 400 MHz): δ_H 2.58 (CH₂-1), 2.62 (CH₂-2), 2.65 (CH₂-3, CH₂-4), 2.69 (CH₂-5, CH₂-6), 2.72 (CH₂-7, CH₂-8). ¹³C{¹H}-NMR (D₂O, 100 MHz): δ_C 40.5 (CH₂-8), 42.5 (CH₂-7), 48.3 (CH₂-6), 50.4 (CH₂-5), 53.2, 53.4 (CH₂-4), 53.8 (CH₂-3), 55.8 (CH₂-2), 58.7, 58.8 (CH₂-1).

mPEG-NH₂: ¹H-NMR (D₂O, 400 MHz): δ_H 3.22 (2H, t, ³J = 5 Hz, -O-CH₂-CH₂-NH₂), 3.39 (3H, s, -O-CH₃), 3.61-3.65 (2H, m, -CH₂-O-CH₃), 3.71 (176H, bs, all the CH₂ groups from the main chain), 3.78 (2H, t, ³J = 5 Hz, -O-CH₂-CH₂-NH₂). ¹³C

{¹H} NMR (D₂O, 100 MHz): δ_C 41.9 (-O-CH₂-CH₂-NH₂), 60.9 (-O-CH₃), 69.1 (-O-CH₂-CH₂-NH₂), 72.3 (all the CH₂ groups from the main chain), 73.8 (-CH₂-O-CH₃).

C60-PEI: ¹H NMR (D₂O, 400 MHz): δ_H 2.67 (bs, CH₂-1, CH₂-2, CH₂-3), 2.74 (bs, CH₂-4, CH₂-5, CH₂-6), 2.81 (bs, CH₂-7, CH₂-8). ¹³C{¹H}-NMR (D₂O, 100 MHz): δ_C 40.4 (CH₂-8), 42.2 (CH₂-7), 48.3 (CH₂-6), 50.2 (CH₂-5), 52.4 (CH₂-4), 53.8 (CH₂-3), 55.6 (CH₂-2), 57.7 (CH₂-1), 130-160 (C60).

C60-PEG-PEI: ¹H NMR (D₂O, 400 MHz): δ_H 2.60 (bs, CH₂-1), 2.64 (bs, CH₂-2), 2.67 (bs, CH₂-3, CH₂-4), 2.72 (bs, CH₂-5, CH₂-6), 2.75 (bs, CH₂-7), 2.76 (bs, CH₂-8), 2.82 (2H, t, ³J = 5.5 Hz, -O-CH₂-CH₂-NH-C60), 3.39 (3H, s, -O-CH₃), 3.59 (2H, t, ³J = 5.4 Hz, -O-CH₂-CH₂-NH-C60), 3.62-3.64 (2H, m, -CH₂-O-CH₃), 3.71 (bs, all the CH₂ groups from the main chain). ¹³C {¹H} NMR (D₂O, 100 MHz): δ_C 40.5 (CH₂-8), 42.5 (CH₂-7 and -O-CH₂-CH₂-NH-C60), 48.4 (CH₂-6), 50.4 (CH₂-5), 53.2 (CH₂-4), 53.9 (CH₂-3), 55.9 (CH₂-2), 58.6 (CH₂-1), 60.8 (-O-CH₃), 72.3 (all the CH₂ groups from the main chain), 73.8 (-CH₂-O-CH₃), 74.5 (-O-CH₂-CH₂-NH-C60), 130-160 (C60).

FTIR Spectroscopy: FTIR spectra were recorded with a Bruker Vertex 70 FT-IR spectrometer, in transmission mode, at 25°C with a resolution of 2 cm⁻¹ and 32 scans. The samples were incorporated in dry KBr pellets. Relative compositions of the samples were estimated quantitatively in 1700-1500 cm⁻¹ interval of FT-IR spectra, by deconvolution of the initial curves, using the Gaussian-Lorentzian function.²⁶

UV-Vis spectroscopy: UV-Vis spectra were recorded with a LAMBDA 35 UV/Vis Systems (Perkin Elmer Inc., USA). The characteristic maxima at 330 nm of UV-Vis absorption of C60 decrease during the conjugation reaction until disappearance. The final products, C60-PEI and C60-PEG-PEI, absorb in the range of 300–700 nm, but no obvious peaks are observed.

Thermal analysis. Thermogravimetric (TG) experiments were conducted on a STA 449 F1 Jupiter device (Netzsch, Germany). 20 mg of each sample was heated in an open alumina crucible, in nitrogen atmosphere, with a flow rate of 50 mL·min⁻¹. A heating rate of 10 °C·min⁻¹ was applied. Samples were heated in the range 30–700 °C. Differential scanning calorimetric (DSC) measurements were conducted on a DSC 200 F3 Maia device (Netzsch, Germany). 10 mg of each sample was heated in punched and sealed aluminum crucibles. A heating rate of 10 °C·min⁻¹ was applied. Nitrogen purge gas was used as inert atmosphere, at a flow rate of 50 mL·min⁻¹. The device was temperature and sensitivity calibrated with indium, according to the standard procedures.

X-ray photoelectron spectrometry-XPS: XPS analyzes were performed on a KRATOS Axis Nova (Kratos Analytical, Manchester, United Kingdom), using AlKα radiation, with 20 mA current and 15 kV voltage (300 W), under a base pressure of 10⁻⁸ to 10⁻⁹ Torr in the sample chamber. The incident monochromatic X-ray beam was focused on a 0.7 mm x 0.3 mm area of the samples bearing surface. XPS survey spectra of PEI, C60-PEI and C60-PEG-PEI were collected in the range of -10 ÷ 1200 eV, with a resolution of 1 eV, at a pass energy of 160 eV. The high resolution spectra for all the elements

identified in the survey spectra were collected using a pass energy of 20 eV and a step size of 0.1 eV. XPS data fitting were performed making use of the Vision Processing software (Vision2 software, Version 2.2.10), and mixed Gaussian-Lorentzian curves. The linear background was subtracted before the peak areas were corrected. The binding energy of the C 1s peak was normalized to 285 eV. Elemental analyzes were performed using a scanning electron microscope (Quanta 200-FEI) equipped with an energy-dispersive X-ray spectroscopy system (EDX). Elemental nitrogen analysis was performed on a Perkin Elmer 2410 Series II CHNS/O ANALYZER 2400.

Atomic Force Microscopy (AFM). The morphology data of polyplexes were obtained using an Ntegra Spectra instrument (NT-MDT, Russia) operated in tapping mode under ambient conditions. Silicon cantilever tips (NSG 10) with a resonance frequency of 140-390 kHz, a force constant of 5.5-22.5 N·m⁻¹ and tip curvature radius of 10 nm were used. To prepare AFM samples, 10 μL aliquotes of polyplexes suspension were deposited on freshly cleaved mica substrate, rinsed with water and dried in air at room temperature. TEM images were obtained on a HT7700 Hitachi Transmission Electron Microscope. The samples were prepared by placing a drop of polyplexes aqueous suspension on a carbon-coated copper grid and by allowing the solvent to evaporate at room temperature. After drying, the samples were examined in high resolution mode, under an operating potential of 100 kV.

Determination of polyplexes size and ζ -potential. The hydrodynamic diameter and ζ -potential of the polymer complexes with salmon sperm DNA were examined using the DelsaNano C Submicron Particle Size Analyzer (Beckman Coulter). The instrument uses photon correlation spectroscopy (PCS), for particle size determinations which consists in measuring the rate of fluctuations in laser light intensity scattered by particles as they diffuse through the fluid, and electrophoretic light scattering (ELS) for zeta potential determination, which determines electrophoretic movement of charged particles under an applied electric field. Light source: Dual 30 mW laser diodes, 658 nm. The size measurements were performed at 25°C and at pH 7.4 and 5.5 in triplicate, and the polyplexes size was evaluated in terms of "number-weighted" distribution. The analysis modes are: CONTIN for size measurements and Smoluchowski for zeta potential.

The DNA binding capacity of C60-PEI and C60-PEI-PEG conjugates was evaluated using the agarose gel retardation assay (the reduction of DNA electrophoretic mobility as a consequence of condensation with polycationic carriers, in direct relationship with the molecular ratio between positive charged amino groups of the carrier, and the negative charged phosphate groups of nucleic acid).^{27,28} Electrostatic polyplexes with different N/P ratios were obtained by mixing salmon sperm dsDNA, and pDNA respectively, with appropriate quantities of C60-PEI, C60-PEG-PEI, or simply PEI (as condensation control; not further discussed), in DNase free 1x TAE buffer solution (pH=7.4). 30 minutes after mixing, the resulted colloidal solutions were loaded in a 1 % agarose gels, and electrophoresis experiments were carried out at 90 V, for 120 minutes, in TAE buffer solution (40 mM Tris-HCl, 1%, acetic acid, 1 mM EDTA). The migration of ds- and p-DNA in

free and complexed states was visualized under UV light, after gels staining with ethidium bromide.

Cell Culture. HEK 293T cells (Human Embryonic Kidney 293T cell line, a kind gift from Professor Dimitris Kardassis, University of Crete, Greece) were incubated at 37 °C and 5 % CO₂ in cell culture plates (12 or 96 wells), using Dulbecco's modified Eagle's medium (DMEM) supplemented with 10 % fetal calf serum (FCS), penicillin (100 U/ml), streptomycin (100 μg/ml) and neomycin (50 μg/ml).

In vitro cytotoxicity assay: The cytotoxicity of uncomplexed PEI, C60-PEI, and C60-PEG-PEI, and their polyplexes with pEYFP plasmid was determined using MTT assay, by measuring the viability of HEK 293T cells, after incubation with the media containing the samples. The method is based on the reduction of a tetrazolium salt (3-[4,5-dimethyl-thiazol-2-yl]-2,5-diphenyltetrazolium bromide, MTT) by the action of dehydrogenase enzymes in metabolically active cells, concluded with the intracellularly generation of purple formazan that can be solubilized and quantified spectrophotometrically.²⁹ HEK 293T cells were seeded in 96-well plates at a density of 5·10³ cells/well, and kept in incubator for 24 h, at 37 °C. Then, the culture media was replaced with fresh medium containing C60-PEI-pEYFP, C60-PEG-PEI-pEYFP or PEI· pEYFP polyplexes, at different N/P ratios, or unloaded C60-PEI, C60-PEG-PEI or PEI conjugates, at the same concentration as the corresponding polyplexes. After 48 hours of incubation at 37°C and 5% CO₂, the liquid was removed from each well, and a solution of 0.5 mg/mL MTT in culture medium was added. After a second incubation of 3 hours at 37°C and 5% CO₂, the resulted formazan crystals were solubilized using a lysis buffer containing 0.1 N HCl in isopropanol, for 4 hours at 37°C. The optical absorbance was measured at 570 nm, with the reference wavelength at 720 nm, using a microplate reader (Tecan GENios). The results were expressed as percentages relative to the results obtained with the control cells (cells incubated in normal cell culture medium).

In vitro transfection efficiency of C60-PEI and C60-PEI-PEG conjugates. Transfection was quantified using the pEYFP, a plasmid encoding the enhanced yellow-green variant of *Aequorea victoria* green fluorescent protein (YFP), which, when excited at 514 nm, emits at 527 nm, with a fluorescence quantum yield of 0.61.³⁰ HEK 293T cells were seeded in 12-well plates at an initial cell density of 1.2·10⁵. After 24 hours, the initial culture medium was replaced by serum-free culture medium containing polyplexes with different well-defined ratios of N/P, at a final concentration of 1 μg pDNA per well, and incubated for 4 hours. After that, serum was added in the incubation medium and the expression of EYFP protein was followed after 48 hours by flow cytometry (using Gallios, Becton Dickinson flow cytometer). As controls, cells incubated with normal cell culture medium (negative control), and cells transfected with plasmid pEYFP DNA using a commercially available transfection reagent (SuperFect® from Qiagen, following the producer's instructions; positive control) were used.

Flow cytometry analysis. Forty eight hours after transfection, HEK 293T cells were harvested using 1.25 % trypsin and analyzed by flow cytometry, to determine the percentage of cells expressing the pEYFP reporter fluorescent protein, and the mean fluorescence intensity (MFI) of EYFP signal. Analysis of green fluorescence from transfected cells was collected in the FL1 channel (530 nm), after excitation with the blue laser (488 nm) of Gallios, Becton Dickinson flow cytometer. The cellular auto-fluorescence was determined using non-transfected cells as control. Transfection efficiency was determined as the percent of EYFP-positive cells relative to the total number of cells investigated by flow cytometer (8000-10000 events counted for each transfection sample). At least 3 independent experiments were performed in duplicate, for each experiment.

Fluorescence microscopy. The expression of pEYFP reporter fluorescent protein in HEK 293T cells was measured 48 hours after the transfection with C60-PEI/pEYFP, C60-PEG-PEI/pEYFP and PEI/pEYFP polyplexes, by fluorescence microscopy, using Olympus IX81 microscope equipped for fluorescence with filter cube for FITC/GFP.

Statistical analysis. Results are presented as means \pm standard error of the mean (SEM). SEM was chosen to evaluate the accuracy of the mean values. Statistical analysis was performed by one-way analysis of variance (ANOVA), and differences were considered significant when $p < 0.05$.

Acknowledgements

This work was supported by a grant of the Romanian National Authority for Scientific Research, CNCS – UEFISCDI, project number PN-II-ID-PCCE-2011-2-0028.

Notes and references

^a "Petru Poni" Institute of Macromolecular Chemistry of Romanian Academy, 41A, Aleea Gr. Ghica Voda, Iasi, Romania.

^b "Nicolae Simionescu" Institute of Cellular Biology and Pathology, Bucharest, 050568, Romania

^c "Gheorghe Asachi" Technical University of Iasi, Iasi, 700050, Romania

^d Institut Européen des Membranes, Adaptive Supramolecular Nanosystems Group - ENSCM-UMII-CNRS UMR- 5635, Place Eugène Bataillon, CC 047, F-34095 Montpellier, Cedex 5, France

[†] The well-defined content of phosphorous in DNA (3 nmol phosphate per 1 μ g DNA) was considered in ratios evaluation. For details see reference 18.

[‡] The exact assignments (shape of the signals and the corresponding number of protons) for individual PEI and for both C60 PEI-containing conjugates, are described only for the proton chemical shifts, extracted from the 2D ¹H-¹³C HSQC spectra.

[§] The ¹H-NMR signal corresponding to -O-CH₂-CH₂-NH-C60 is shifted from 3.78 ppm, in the mPEG-NH₂ spectrum, to 3.59 ppm, in C60-PEG derivative, and the one associated to -O-CH₂-CH₂-NH-C60 is shifted from 3.22 to 2.82 ppm.

[§] The ¹³C-NMR signal corresponding to -O-CH₂-CH₂-NH- is shifted from 69.1 ppm, in PEG spectrum, to 74.5 ppm, in C60-PEG derivative. Correspondingly, the signal of -O-CH₂-CH₂-NH- is shifted from 41.9 to 42.5 ppm.

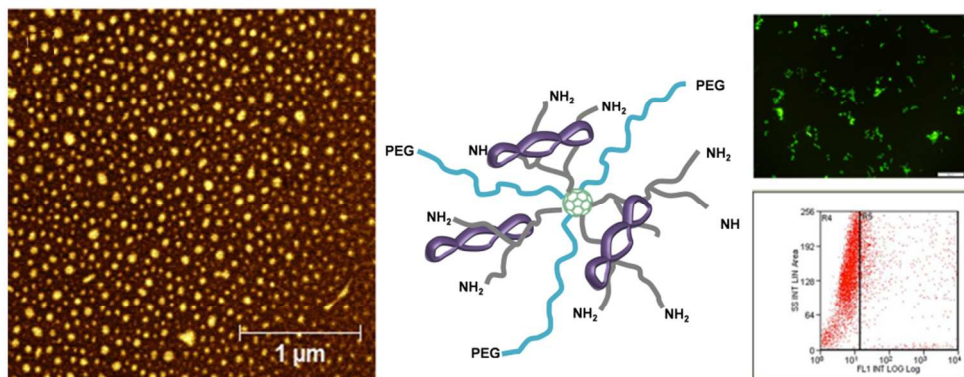
Electronic Supplementary Information (ESI) available: Synthetic details, supplementary NMR, FTIR, UV-VIS, XPS spectra, thermal analyses and

transfection efficiency details are supplied as ESI. See DOI: 10.1039/b000000x/

- W.Y. Yuting, S. Pan, X. Luo, X. Zhang, W. Zhang, M. Feng, *Bioconjugate Chem.* 2009, **20**, 322-332.
- M. Neu, D. Fisher, T. Kissel, *J. Gene Med.* 2005, **7**, 992-1009.
- R. Deng, Y. Yue, F. Jin, Y. Chen, H.-F. Kung, M. C. M. Lin, C. Wu, *J. Control. Release* 2009, **140**, 40-46.
- a) M. L. Forrest, J. T. Koerber, D.W. Pack *Bioconjugate Chem.* 2003, **14**, 934-940; b) U. Rungsardthong, M. Deshpande, L., Bailey, M. Vamvakaki, S.P. Armes, M.C. Garnett, S. Stolnik, *J. Control. Release* 2001, **73**, 359-380.
- a) A. Montellano, T. Da Ros, A. Bianco, M. Prato *Nanoscale*, 2011, **3**, 4035-4041 and references therein; b) C.O. Mellet, J.M. Benito, J.M. Garcia Fernandez *Chem Eur J.* 2010, **16**, 6728-6742; c) M. Pinteala, A. Dascalu, C. Ungureanu, *Int. J. Nanomed.* 2009, **4**, 193-199.
- H. S. Lai, W. J. Chen, L. Y. Chiang, *World J. Surg.* 2000, **24**, 450-454.
- H. Jin, W. Q. Chen, X. W. Tang, L. Y. Chiang, C. Y. Yang J. V. Schloss, J. Y. Wu, *J. Neurosci. Res.* 2000, **62**, 600-607.
- L. L. Dugan, E. G. Lovett, K. L. Quick, J. Lotharius, T. T. Lin, K. L. O'Malley, *Parkinsonism Relat. D.* 2001, **7**, 243-246.
- M.P. Gelderman, O. Simakova, J. D. Clogston, A. K. Patri, S. F. Siddiqui, A. C. Vostal, J. Simak, *Int. J. Nanomed.* 2008, **3**, 59-68.
- J. J. Yin, F. Lao, J. Meng, P.P. Fu, Y. Zhao, G. Xing, X. Gao, B. Sun, P.C. Wang, C. Chen, X.J. Liang, *Mol. Pharmacol.* 2008, **74**, 1132-1140.
- Y. Mikata, S. Takagi, M. Tanahashi, S. Ishii, M. Obata, Y. Miyamoto, K. Wakita, T. Nishisaka, T. Hirano, T. Ito, M. Hoshino, C. Ohtsuki, M. Tanihara, S. Yano, *Bioorg. Med. Chem. Lett.* 2003, **13**, 3289-3292.
- a) R. Seshadri, A. Govindaraj, R. Nagarajan, T. Pradeep, C. N. R. Rao, *Tetrahedron Lett.* 1992, **33**, 2069-2070; b) N. Manolova, L. Rashkov, F. Beguin, H. van Damme, *J. Chem. Soc., Chem. Comm.* 1993, 1725-1727.
- a) E. Nakamura, H. Isobe, H. Tomita, M. Sawamura, S. Jinno, H. Okayama, *Angew. Chem. Int. Ed.* 2000, **39**, 4254-4257; b) D. Sigwalt, M. Holler, J. Iehl, J.-F. Nierengarten, M. Nothisen, E. Morin, J.-S. Remy, *Chem. Commun.*, 2011, **47**, 4640-4642; c) R. Maeda-Mamiya, E. Noiri, H. Isobe, W. Nakanishi, K. Okamoto, K. Doi, T. Sugaya, T. Izumi, T. Homma, E. Nakamura, *Proc. Natl. Acad. Sci. U. S. A.*, 2010, **12**, 5339-5344; d) I. Nierengarten J.-F. Nierengarten *Chem. Asian J.* 2014, **9**, 1436 – 1444
- M. Das, R. Jain, A.K. Agrawal, K. Thanki, S. Jain, *Bioconjugate Chem.* 2014, **25**, 501-509.
- C.L. Chan, R.N. Majzoub, R.S. Shirazi, K.K. Ewert, Y.J. Chen, K.S. Liang, C.R. Safinya, *Biomaterials* 2012, **33**, 4928-4935.
- S.-J. Sung, S.H. Min, K.Y. Cho, S. Lee, Y.-J. Min, Y.I. Yeom, J.-K. Park, *Biol. Pharm. Bull.* 2003, **26**, 492-500.
- X. Zhang, S.-R. Pan, H.-M. Hu, G.-F. Wu, M. Feng, W. Zhang, X. Luo, *J. Biomed. Mater. Res. A.* 2008, **84**, 795-804.
- B.A. Demeneix, M. Ghorbel, D. Goula, *Methods in Molecular Biology*, E.B. Kmiec, Ed., Humana Press Inc., Totowa, NJ, **2000**. Vol. 133: Gene Targeting Protocols, pp 21-35.
- R. Kircheis, L. Wightman, A. Schreiber, B. Robitzka, V. Rössler M. Kurska, E. Wagner, *Gene Ther.* 2001, **8**, 28-40.
- D. M. Tzirakis, M. Orfanopoulos, *Chem Rev.* 2013, **113**, 5262-5321.
- G. P. Miller, *C. R. Chim.* 2006, **9**, 952-959.
- J. Shi, H. Zhang, L. Wang, L. Li, H. Wang, Z. Wang, Z. Li, C. Chen, L. Hou, C. Zhang, Z. Zhang, *Biomaterials* 2013, **34**, 251-261.
- H. Liu, H. Wang, W. Yang, Y. Cheng *J. Am. Chem. Soc.* 2012, **134**, 17680-17687.

24. For Dynamers see: a) W.G. Skene, J. M. Lehn, *Proc. Natl. Acad. Sci.* 2002, **99**, 8270-8275; b) J. M. Lehn, *Prog. Polym. Sci.* 2005, **30**, 814-831; c) L. Marin, B. Simionescu, M. Barboiu, *Chem. Commun.* 2012, **48**, 8778-8780; d) L. Marin, S. Moraru, M.-C. Popescu, A. Nicolescu, C. Zgardan, B. C. Simionescu, M. Barboiu, *Chem. Eur. J.* 2014, **20**, 4814-4821.
25. For Dynamic Reversible Frameworks see : a) G. Nasr, A. Gilles, T. Macron, C. Charmette, J. Sanchez, M. Barboiu, *Israel J. Chem.* 2013, **53**, 97-101; b) G. Nasr, T. Macron, A. Gilles, C. Charmette, J. Sanchez, M. Barboiu, *Chem. Commun.* 2012, **48**, 11546-11548; c) G. Nasr, T. Macron, A. Gilles, Z. Mouline, M. Barboiu, *Chem. Commun.* 2012, **48**, 6827-6829; d) G. Nasr, T. Macron, A. Gilles, E. Petit, M. Barboiu, *Chem. Commun.* 2012, **48**, 7398-7400.
26. V. A. Lórenz-Fonfría, E. Padrós, *Spectrochim. Acta A* 2004, **60**, 2703-2710.
27. Y. Chen, W. Wang, G. Lian, C. Qian, L. Wang, L. Zeng, C. Liao, B. Liang, B. Huang, K. Huang, *Int. J. Nanomed.* 2012, **7**, 359-367.
28. L. Novo, E. Mastrobattista, C. F. van Nostrum, W. E. Hennink, *Bioconjugate Chem.* 2014, **25**, 802-812.
29. J. C. Stockert, A. Blázquez-Castro, M. Cañete, R. W. Horobin, Á. Villanueva, *Acta Histochem.* 2012, **114**, 785-796.
30. S. G. Olenych, N. S. Claxton, G. K. Ottenberg, M. W. Davidson, *Curr. Protoc. Cell. Biol.* 2007, Chapter 21, Unit 21.5.

C60-PEI and C60-PEG-PEI conjugates act as efficient binders of double stranded DNA (dsDNA) polyplexes that exhibit good transfection efficiency and are performant in terms of expression of EYFP reporter gene in cultured cells and exhibited high cytocompatibility, determining cell proliferation up to 200%.



191x78mm (144 x 144 DPI)